

Climate of the Past Discussions is the access reviewed discussion forum of *Climate of the Past*

Numerical reconstructions of the Northern Hemisphere ice sheets through the last glacial-interglacial cycle

S. Charbit¹, C. Ritz², G. Philippon¹, V. Peyaud², and M. Kageyama¹

¹LSCE/IPSL, CEA-CNRS-UVSQ, UMR 1572, CE Saclay, Orme des Merisiers, Bat. 701, 91191 Gif-sur-Yvette cedex, France

²LGGE, CNRS, 54, rue Molière-BP96, 38402 Saint Martin d'Hères cedex, France

Received: 28 August 2006 – Accepted: 19 September 2006 – Published: 26 September 2006

Correspondence to: S. Charbit (sylvie.charbit@cea.fr)

CPD

2, 879–921, 2006

Ice-sheet evolution during the last climatic cycle

S. Charbit et al.

Title Page

Abstract

Introduction

Conclusions

References

Tables

Figures

⏪

⏩

◀

▶

Back

Close

Full Screen / Esc

Printer-friendly Version

Interactive Discussion

EGU

Abstract

A 3-dimensional thermo-mechanical ice-sheet model is used to simulate the evolution of the Northern hemisphere ice sheets through the last glacial-interglacial cycle. The ice-sheet model is forced by the results from six different atmospheric general circulation models (AGCMs). Two climate snapshots simulations performed for the last glacial maximum (LGM) and for the present-day periods are interpolated through time using a glacial index calibrated against the GRIP $\delta^{18}\text{O}$ record to reconstruct the climate evolution over the period under study. Since it is driven by the timing of the GRIP signal, the temporal evolution of the ice volume and the ice-covered area is approximately the same from one simulation to the other. However, both ice volume curves and spatial distributions of the ice sheets present some major differences from one AGCM to the other. The origin of these differences, which are most visible in the maximum amplitude of the ice volume, is analyzed in terms of differences in climate forcing. The analysis of the results allows an evaluation of the ability of GCMs to simulate climates consistent with the reconstructions of past ice sheets to be evaluated. Although some models properly reproduce the advance or retreat of ice sheets in some specific areas, none of them is able to reproduce both North American or Eurasian ice complexes in full agreement with observed sea-level variations and geological data. These deviations can be attributed to shortcomings in the climate forcing and in the LGM ice-sheet reconstruction used as a boundary condition for GCM runs, but also to missing processes in the ice-sheet model itself.

1 Introduction

In addition to Greenland and Antarctica, massive ice complexes covering North America (Laurentide and Cordillera) and the northern part of the Eurasian continent (Fennoscandia) developed during the last glacial cycle. The sea-level history inferred from coral dating (Bard et al., 1990, 1996; Fairbanks, 1989) or the isotopic signals

CPD

2, 879–921, 2006

Ice-sheet evolution during the last climatic cycle

S. Charbit et al.

Title Page

Abstract

Introduction

Conclusions

References

Tables

Figures

◀

▶

◀

▶

Back

Close

Full Screen / Esc

Printer-friendly Version

Interactive Discussion

EGU

recorded in marine sediments (Bond et al., 1993; Waelbroeck et al., 2002) or ice cores (Andersen et al., 2004; Johnsen et al., 1995) have revealed that this period was characterized by several phases of growth and retreat of the ice sheets.

During the Last Glacial Maximum (LGM) and the subsequent deglacial period, the areal extent of the North American ice sheet is quite well constrained (Clark et al., 1993; Dyke and Prest, 1987). Moreover a reconstruction of the maximum limits of the Eurasian ice sheet for the Late Quaternary period, based on satellite observations of geomorphological features, aerial photographs and various types of geological data has recently been published (Svendsen et al., 2004) within the framework of the QUEEN project (Quaternary Environments of the Eurasian North project). However, as often outlined (Kleman et al., 2002; Marshall, 2002; Zweck and Huybrechts, 2005), large uncertainties remain about the shape, the volume and the thickness of these former ice sheets, and their evolution through time. The best way for these characteristics to be better constrained is the use of numerical modeling. In this view, several approaches have been followed during the past decade. The first one relies on glacio-hydro-isostasy models based on relative sea-level observations that account for the temporal evolution of the ice load and the subsequent rheological response of the geoid to surface loading. These models provide an estimate of either the global ice volume at the LGM (Milne et al., 2002; Yokoyama et al., 2000) or a reconstruction of the ice volume equivalent sea-level during the deglacial history (Lambeck et al., 2000, 2002) or prior to the LGM (Lambeck and Chappell, 2001). Similar models constrained both by sea-level datasets and by geological reconstructions of the ice margins are designed to give a 3-D picture of individual ice sheet (Lambeck, 1995; Peltier, 1994, 2004). However, these latter approaches only provide ice-sheet reconstructions during the deglacial period, and not prior the LGM; moreover in regions in which data is unavailable, the ice thickness is often under-constrained.

A second alternative consists in using ice-sheet models. Two approaches have generally been followed. The first one relies on simplified climate models (energy balance models or Earth climate models of intermediate complexity) coupled to 2-D vertically

Ice-sheet evolution during the last climatic cycle

S. Charbit et al.

Title Page

Abstract

Introduction

Conclusions

References

Tables

Figures

◀

▶

◀

▶

Back

Close

Full Screen / Esc

Printer-friendly Version

Interactive Discussion

integrated ice-sheet models (e.g., Deblonde and Peltier, 1991; Deblonde et al., 1992; Gallée et al., 1992; Marsiat, 1994; Peltier and Marshall, 1995; Tarasov and Peltier, 1997). The second approach is based on the use of 3-D dynamical ice-sheet models asynchronously coupled to an EBM (Tarasov and Peltier, 1999) or used in a forced mode. In this latter case, the climate forcing can simply be derived from ice core data (Greve et al., 1998; Huybrechts, 2002; Ritz et al., 1997) or from GCM climate snapshots interpolated through time using a glacial index generally inferred from the GRIP $\delta^{18}\text{O}$ signal (Charbit et al., 2002; Marshall et al., 2002, 2000; Tarasov and Peltier, 2004; Zweck and Huybrechts, 2005).

Studies based on simplified climate and/or ice-sheet models generally aim at examining which kind of processes enable a reasonable simulation of the ice volume through the last glacial-interglacial cycle. Although the global ice volume at the LGM is generally quite well reproduced, the reconstruction of the spatial distribution of the individual ice masses and their specific shape often suffers from major drawbacks such as an insufficient southward extent of the North American ice sheet (Deblonde and Peltier, 1991; Gallée et al., 1992; Marsiat, 1994), an erroneous simulation of the Eurasian sector (Deblonde and Peltier, 1991; Deblonde et al., 1992; Tarasov and Peltier, 1997), a too much extended ice-covered area over Alaska, and the growth of ice in the Siberian region (Deblonde et al., 1992; Marsiat, 1994; Peltier and Marshall, 1995). These models often fail in successfully simulating the deglaciation process without incorporating any ad hoc process (Deblonde and Peltier, 1991; Gallée et al., 1992; Peltier and Marshall, 1995).

The evolution of ice sheets during the last glacial cycle is expected to be in a better agreement with geological data when using 3-D thermomechanical ice-sheet models. However, large differences are observed between the results provided, as an example, by the studies of Tarasov and Peltier (1999), Marshall et al. (2000), Bintanja et al. (2002) or Zweck and Huybrechts (2005). These differences appear in the magnitude and in the timing of the maximum ice volume, in the ice thickness and more generally in the shape of the ice sheets, in the repartition of ice between Eurasia and North America,

Ice-sheet evolution during the last climatic cycle

S. Charbit et al.

Title Page

Abstract

Introduction

Conclusions

References

Tables

Figures

◀

▶

◀

▶

Back

Close

Full Screen / Esc

Printer-friendly Version

Interactive Discussion

in the erroneous simulation of ice over Alaska and Siberia, and finally in the timing of the deglaciation process.

The different sources of uncertainties may come from the climate reconstruction used to force the ice-sheet model, that is from the climate model or from the basis of the climatic index method and finally from the choice of the index itself. It has been demonstrated that the use of climatic outputs coming from 17 GCMs leads to considerable scatter in the computed mass balance of the ice sheets (Pollard and Group, 2000). The second cause which may be at the origin of the discrepancies between the results provided by different groups lies in the choice of the ice-sheet model, or more specifically in the choice of some physical parameters related to ice flow, that are under-constrained (Marshall et al., 2002).

In this paper we focus on the uncertainties linked to the climate forcing. To this end we used climatic outputs from different atmospheric general circulation models (AGCMs) involved in the first Paleoclimate Modelling Intercomparison Project (PMIP, Joussaume and Taylor, 1995) to force a single 3-D ice-sheet model of the Northern hemisphere. Among the 22 PMIP models, only 10 of them provided snapshot climate simulations of the LGM and the present-day periods with fixed sea surface temperatures (SSTs) and sea ice cover. We removed from our selection the older version of the GCM developed at the Laboratoire de Météorologie Dynamique (i.e. LMD4), as well as the model which has the lowest resolution. For the present study, we chose six of the eight remaining models to keep a representative range of spatial horizontal resolutions of the PMIP-GCMs.

The aim of the present study is twofold. First it is to document the differences between the simulated spatial distributions of the ice sheets and the evolution of the ice volumes. Secondly it is to investigate whether climate forcings produced by the PMIP-GCMs are able to produce ice sheets in agreement with geological data and observed sea-level variations, and whether the LGM ice sheets are consistent with the reconstruction used as a boundary condition for the LGM GCM runs.

Ice-sheet evolution during the last climatic cycle

S. Charbit et al.

Title Page

Abstract

Introduction

Conclusions

References

Tables

Figures

◀

▶

◀

▶

Back

Close

Full Screen / Esc

Printer-friendly Version

Interactive Discussion

2 Description of the approach

2.1 The ice-sheet model

A full description of GREMLINS (GREnable Model of Land Ice of the Northern hemisphere) can be found in Ritz et al. (1997). In the present paper we just recall the main characteristics of the model. It is a three-dimensional thermomechanical ice-sheet model which predicts the evolution of the geometry (extension and thickness) of the ice and the coupled temperature and velocity fields. This model only accounts for grounded ice without incorporating a description of ice flow through ice streams and does not deal with ice shelves. The equations are solved on a Cartesian grid (45 km×45 km) corresponding to 241×231 grid points of the northern hemisphere. The evolution of the ice sheet surface and geometry is a function of surface mass balance, velocity fields, and bedrock position. The isostatic adjustment of bedrock in response to the ice load is governed by the flow of the asthenosphere with a characteristic time constant of 3000 years, and by the rigidity of the lithosphere. The temperature field is computed both in the ice and in the bedrock by solving a time-dependent heat equation. Changes in the ice thickness with time are computed from a continuity equation and are a function of the ice flow, the surface mass balance and the basal melting. The ice flow results both from internal ice deformation and basal sliding. It is calculated with the zero-order shallow ice approximation. The surface mass balance is the sum of accumulation and ablation, both of which depending on surface air temperature (colder air leads to increased aridity). The accumulation term is inferred from the AGCM mean annual air temperature and total precipitation fields. The fraction of solid precipitation is considered to be proportional to the fraction of the year with mean daily temperature less than 2°C. The mean daily temperature is computed from mean annual and summer (June–August) air temperatures provided by the GCM. We use the mean annual and summer AGCM fields, and the seasonal cycle is reconstructed assuming a sine wave with the amplitude given by the difference between summer and annual temperatures. The ablation term is computed using the positive-degree-day (PDD) method,

CPD

2, 879–921, 2006

Ice-sheet evolution during the last climatic cycle

S. Charbit et al.

Title Page

Abstract

Introduction

Conclusions

References

Tables

Figures

◀

▶

◀

▶

Back

Close

Full Screen / Esc

Printer-friendly Version

Interactive Discussion

EGU

which is based on an empirical relation between air temperatures and melt processes. In the present study, this method is used exactly as the same way as described in Reeh (1991) and accounts for albedo differences between snow and ice and for the production of superimposed ice due to meltwater that refreezes.

5 2.2 The forcing method

The forcing method is explicitly described in Charbit et al. (2002). In this section we summarize its basic principles. Due to their high computational cost, the general circulation models can only provide snapshots of climate. Hence, we used two climate snapshots, one for a glacial period, the Last Glacial Maximum (21 kyr BP), and one for the present-day period, representing two extreme climates of the last glacial-interglacial cycle. To obtain a time-dependent climatology over the entire cycle, the AGCM fields used to drive the ice-sheet model are interpolated through time (see below). These fields are the 2-m mean annual and summer surface air temperatures and the annual precipitation and they are used to compute both ablation and accumulation. To minimize the errors due to GCM deficiencies, we use a perturbative method of the present-day climate: the anomaly fields are computed as a difference for temperature and as a ratio for precipitation between simulated control (“ctrl”) and past (“paleo”) climates (Fig. 1). As these variables are strongly influenced by local topography, corrections of precipitation are required to account for surface elevation difference between the GCM and the ice-sheet model. For temperature, we apply a vertical gradient derived from empirical observations in Greenland (Ohmura and Reeh, 1991): 8°C/km and 6.5°C/km for annual and summer temperature. To account for less moisture at high altitude we assume that precipitation is exponentially dependent on temperature. Therefore a difference of temperature corresponds to a ratio of precipitation. The corrected AGCM anomalies $\Delta T_{\text{cor}}(t)$ and $\Delta P_{\text{cor}}(t)$ can be written as:

$$\Delta T_{\text{cor}}(t) = (T_{\text{paleo}} - T_{\text{ctrl}})(t) + \lambda \cdot (S_{\text{paleo}} - S_{\text{ctrl}})$$

Ice-sheet evolution during the last climatic cycle

S. Charbit et al.

Title Page

Abstract

Introduction

Conclusions

References

Tables

Figures

◀

▶

◀

▶

Back

Close

Full Screen / Esc

Printer-friendly Version

Interactive Discussion

Ice-sheet evolution during the last climatic cycle

S. Charbit et al.

$$\Delta P_{\text{cor}}(t) = \exp(0.05 \times (T_{\text{ctrl}} - T_{\text{paleo}})) \times \frac{P_{\text{paleo}}}{P_{\text{ctrl}}}(t)$$

where T , P , S and λ are related to temperature, precipitation, surface elevation and vertical lapse rate. The exponential term in the anomaly of precipitation accounts for all processes that are linked to a difference of temperature between past and present. The numerical value 0.05 is deduced from the temperature-precipitation relationship in the same way as in Charbit et al. (2002). These anomalies are then interpolated on the ice-sheet model (ISM) grid. The time-dependent climatology is obtained by interpolating through time these latter anomalies using a climatic index inferred from the $\delta^{18}\text{O}$ GRIP record, so that at each time step, the climatic fields used to force GREMLINS can be expressed with:

$$\Delta X_{\text{ISM}}(t) = (1 - \alpha(t))\Delta X_{\text{LGM}}$$

where the α coefficient represents the proportion of interglacial climate ($\alpha=0$ for the LGM and $\alpha=1$ for the present-day period), and ΔX_{LGM} stands for the corrected anomaly of temperature or precipitation. This approach is similar to the one previously used by Marshall et al. (2000) or Charbit et al. (2002). The main assumption is that the spatial patterns of temperature or precipitation variations (i.e. between past and present) do not change with time, and that the climatic variations are only driven by the temporal variations of the α coefficient. The temperature at the surface of the ice-sheet model (T_{rec}) is reconstructed at each time step from the resulting anomaly $\Delta T_{\text{ISM}}(t)$ added to the present-day climatology (T_{clim}) and a corrective factor accounting for the surface elevation difference between past and present:

$$T_{\text{rec}} = T_{\text{clim}} - \lambda(S_{\text{paleo,ISM}} - S_{\text{ctrl,ISM}}) + \Delta T_{\text{cor}}(t)$$

In the same way, the reconstructed precipitation is derived from the product of $\Delta P_{\text{ISM}}(t)$ and the observed precipitation. The impact of the temperature difference between past and present is accounted for by the exponential term:

$$P_{\text{rec}} = P_{\text{clim}} \times \exp(0.05 \times (T_{\text{rec}} - T_{\text{clim}})) \times \Delta P_{\text{cor}}(t)$$

[Title Page](#)
[Abstract](#)
[Introduction](#)
[Conclusions](#)
[References](#)
[Tables](#)
[Figures](#)
[◀](#)
[▶](#)
[◀](#)
[▶](#)
[Back](#)
[Close](#)
[Full Screen / Esc](#)
[Printer-friendly Version](#)
[Interactive Discussion](#)

The present-day topography is based on the GLOB-ETOPO2 dataset and the Greenland bedrock has been elaborated by Bamber et al. (2001).

The present-day climatology is based on the ERA-40 re-analyses for the temperature fields. The precipitation is derived from a compilation between the CRU dataset over continents (New et al., 1999) and the GPCP dataset over oceans (Adler et al., 2003). Moreover, for the Arctic area, the precipitation data is provided by Serreze and Hurst (2001).

It is worth noting that owing to the fact GREMLINS is not fully coupled to the GCMs, the present approach cannot account for the changes in atmospheric circulation and in the albedo effect due to changes in the ice sheets geometry. Other artefacts are also introduced by using LGM climate snapshots which strongly influences our representation of past climate throughout the last glacial-interglacial cycle by overestimating the albedo effect in regions which were covered by snow at the LGM. In the following, we call this effect the “artefact albedo effect”.

2.3 The experimental set-up

The specificities of the AGCM runs used in this study are summarized in Table 1. All the six models used in this study have been forced by i) the insolation at the top of the atmosphere (Berger, 1978), ii) the atmospheric CO₂ inferred from ice core measurements (Raynaud et al., 1993), iii) the prescribed seasonally varying sea surface temperatures and the sea-ice cover, both derived from the CLIMAP dataset (CLIMAP, 1981) for the LGM climate and from observations for the control run (i.e. present-day run), iv) the LGM sea-level lowering and the ice-sheet geometry (extent and altitude) obtained from the LGM ICE-4G reconstruction (Peltier, 1994) and from the observations for the present-day climate. For the UGAMP and the GENESIS2 models the SSTs from the CLIMAP reconstruction have been directly used as boundary conditions for the LGM run, while for the other models (ECHAM3, LMD5, MRI2 and CCSR1) the prescribed SSTs are reconstructed from the CLIMAP (1981) changes between past and present added to the present-day observations used for the control run. In the same way, for

Ice-sheet evolution during the last climatic cycle

S. Charbit et al.

Title Page

Abstract

Introduction

Conclusions

References

Tables

Figures

◀

▶

◀

▶

Back

Close

Full Screen / Esc

Printer-friendly Version

Interactive Discussion

all models, the ice-sheet topography is given by the topography anomaly between past and present obtained from the differences between the LGM and the present-day ICE-4G reconstructions (Peltier, 1994), added to the present-day topography coming from the observations (see Table 1).

5 Although the analyses presented in this paper are focused on the last glacial cycle (130–0 kyr BP), the ice-sheet model is run during 230 kyr for model spin-up. This procedure is necessary to obtain a reasonable vertical profile of temperature in the ice, and to a lesser extent, to integrate the history of the bedrock response to changes in surface loading. The initial topography is given by the present-day topography and the
10 climate forcing is obtained from the method previously described.

3 Results

3.1 Spatial distribution

Time slices of the simulated spatial distributions of the ice sheets are represented in Figs. 3–7 at different key periods of the last glacial cycle. These maps exhibit great
15 differences both in altitude and ice-covered areas from one simulation to the other. Although our discussion mainly focuses on the simulated North American and Eurasian ice sheets, it is worth noting that differences are also observed in the extent and the altitude of the Greenland ice sheet throughout the simulation. However, at the present day period (Fig. 7), the six experiments are in a full agreement concerning the extent of
20 Greenland and its ice thickness and match with observations. Moreover, the simulated American and Eurasian ice sheets have almost completely melted, although small ice masses are still present over the Baffin Island and the Arctic Ocean.

3.1.1 The North American ice sheet

The most important point at the early phase of glaciation (113 kyr BP, Fig. 3) is related to the location of the inception sites. All models produce ice over the Canadian
25

Ice-sheet evolution during the last climatic cycle

S. Charbit et al.

Title Page

Abstract

Introduction

Conclusions

References

Tables

Figures

◀

▶

◀

▶

Back

Close

Full Screen / Esc

Printer-friendly Version

Interactive Discussion

Archipelago, the Baffin Island and over the Northern Rocky Mountains. In the simulations performed with GENESIS2, UGAMP and CCSR1 ice also covers the Keewatin region, while small ice caps are produced in the Labrador sector with LMD5 and CCSR1, and in the Hudson Bay lowland with CCSR1 and UGAMP. Observational data (Andrews and Barry, 1978) indicate that the regions of ice-sheet inception in North America were those bordering the eastern coast, such as the Baffin Island and the Quebec-Labrador region, as well as the uplands of Northeastern Keewatin. This is concordant with our reconstructions, except for the Labrador sector where small ice caps are only produced with two models. Moreover, the advance of ice in the Middle West region is highly discordant with the geological data. The excess of ice in this area, simulated by using UGAMP outputs as climate forcing, seems to be directly related to a high precipitation ratio added to a small anomaly of temperature. Paleoenvironmental records indicate that, at the early beginning of the glaciation, climate in the Rocky Mountains regions was as warm as, or warmer than present (Clark et al., 1993). Hence, the Cordilleran ice sheet does not appear to have developed before the late isotopic stage 5 or 4 (i.e. ~75 kyr BP). At that time, the ice advanced over the Southern British Columbia and into the Northern Puget lowland, whereas northern areas were later covered by ice, which is in contradiction with our modeling results. This discordance can be explained by the shortcomings of our approach. Actually, according to a study carried out by Clark and Bartlein (1995), the Cordilleran ice sheet started to grow when the Laurentide ice sheet was high enough to induce a displacement of the jet stream causing precipitation to fall over the Rocky Mountains. Such a glaciation sequence cannot be represented with our methodology because it does not account for the feedbacks of the ice sheets on the atmospheric circulation. Moreover, the use of LGM climate snapshots in the climate forcing induces an artefact albedo effect (see Sect. 2.2) in regions covered by snow at the LGM, and hence favours the glaciation LG process at any time of the last glacial-interglacial cycle.

The results obtained for the 112 kyr BP period (Fig. 4) confirm that for the CCSR1 model the regions of early glaciation (Labrador-Quebec, Rockies and Keewatin) coa-

Ice-sheet evolution during the last climatic cycle

S. Charbit et al.

Title Page

Abstract

Introduction

Conclusions

References

Tables

Figures

◀

▶

◀

▶

Back

Close

Full Screen / Esc

Printer-friendly Version

Interactive Discussion

lesce to form the North American ice sheet. A dome develops over South Keewatin in the simulation performed with the UGAMP model and ice has coalesced with that covering the Northern part of the ice sheet and that spreading over the Cordilleran region. The western sector of the Laurentide ice sheet, as well as the Labrador and the Rocky Mountains regions, have widely extended compared to the 113 kyr BP period (Fig. 3). The rapid expansion of the ice is probably due to the artefact albedo effect due to the use of LGM climate snapshots, as previously mentioned. The simulations performed with ECHAM3 and GENESIS2 are characterized by an expansion of ice in the Middle West region, whereas for the MRI2 model, the only ice-covered area is the Northern part of Canada.

According to the ice volume curves (Fig. 8) the full glacial period starts after the last major phase of glaciation at around 57 kyr BP (Fig. 5). These maps indicate that the largest differences from one model to the other concern the shape of the North American ice sheet, the extent of Fennoscandia (see following section) and the presence of ice in Alaska and Siberia. According to geological records, the inception of ice in Keewatin and in the Quebec-Labrador Plateau leads to the coalescence of both ice masses and to the formation of two domes centred on these sectors. However, none of the simulations presented in the present study is able to reproduce the Keewatin dome. This is partly due to the fact that this dome is not represented in the LGM ICE-4G reconstruction (Fig. 2) used as a boundary condition for the GCM simulations. The second deviation from geological records concerns the Cordilleran ice sheet; as outlined in the synthesis provided by Clark et al. (1993), the ice sheet was only a little more extensive than today during its first phase of development, and completely disappeared before the end of stage 4 (~59 kyr BP). It then started to readvance by 25–30¹⁴C kyr BP (i.e. 29–34 kyr BP, after Bard et al., 2004), in response to a new climatic deterioration to reach its maximum extent at around 15–14¹⁴C kyr BP (i.e. 16–18.5 kyr BP, after INTCAL04 from Reimer et al., 2004). Our modeling results are highly discordant from such a configuration. First, the Cordilleran region remains glaciated throughout the simulated last glacial period whatever the choice of the forcing GCM, and starts to

Ice-sheet evolution during the last climatic cycle

S. Charbit et al.

Title Page

Abstract

Introduction

Conclusions

References

Tables

Figures

⏪

⏩

◀

▶

Back

Close

Full Screen / Esc

Printer-friendly Version

Interactive Discussion

retreat synchronously with the Laurentide ice sheet. The other point of disagreement lies in a too large ice extent in Alaska. As reminded by Clague and James (2002), the Cordilleran ice sheet was only extended over the southern part of this region and consisted in small ice fields and glaciers flowing towards the Pacific Ocean or the Yukon River (Mann and Hamilton, 1995). Consequently much of the Alaskan interior likely remained to be unglaciated throughout the last glacial cycle. In the present study, the use of CCSR1, UGAMP and even MRI2 and GENESIS2 probably overestimate the amount of ice over Alaska, whereas LMD5 and ECHAM3 are presumably in a better agreement with data.

The last point which could be discussed is related to the coalescence of the Cordilleran and Laurentide ice sheets. There is no complete consensus about the junction or the separation of these ice sheets. At present, some groups pretend that the coalescence did not occur all along the north-south transect at the frontier between the Cordilleran and Laurentide ice sheets (see Dyke et al., 2002, for a detailed review), while Dyke et al. (2002) support the idea that they were fully coalescent at the LGM because it is difficult to conceive that the ice sheets were joined in some places and not in other. This is in agreement with the LGM ICE-4G reconstruction (Peltier, 1994) which does not reproduced a separation between the ice sheets (Fig. 2), although the ice thickness is smaller than in the adjacent regions. However, the use of the GENESIS2 climatic outputs allows a disconnection between the ice sheets to be clearly simulated at the LGM (Fig. 6), due to the fact that at the frontier between Cordillera and Laurentide, simulated surface temperatures are warmer than in the surroundings. Other deviations from the ICE-4G reconstruction (Fig. 2) are observed in our LGM simulations. First, the southern margin is too much extended in some models (CCSR1, UGAMP and ECHAM3). Except for ECHAM3 and LMD5, the ice extent in Alaska is overestimated and the advance of ice in the Baffin Bay is not properly reproduced with the use of MRI2, GENESIS2 and LMD5, due partly to summer temperatures in this region warmer than those simulated by the three other models. Finally, the maximum ice thickness is not located at the same place than in ICE-4G.

Ice-sheet evolution during the last climatic cycle

S. Charbit et al.

Title Page

Abstract

Introduction

Conclusions

References

Tables

Figures

◀

▶

◀

▶

Back

Close

Full Screen / Esc

Printer-friendly Version

Interactive Discussion

3.1.2 The Eurasian ice sheet

The glaciation over the Eurasian continent starts with small ice caps formed over the Taimyr Peninsula and some Arctic islands (Figs. 3–4). This is in accordance with the recent review performed within the framework of the QUEEN project (Svendsen et al., 2004). The formation of ice is also simulated in the Norwegian mountains as early as 113 kyr BP (Fig. 3) with all models except LMD5 because of a relatively high annual summer surface air temperature. By 112 kyr BP (Fig. 4), the ice-covered areas have significantly extended. The most rapid expansion of ice can be seen with ECHAM3 and UGAMP, and to a lesser extent with CCSR1, with significant amounts of ice east of the Taimyr Peninsula and close to Eastern Siberia. Although there is few data related to the early glaciation of Eurasia, there is no geological record indicating that there was ice in these latter regions. However, the presence of ice in Siberia could be a direct consequence of the albedo effect induced by the marine ice mass in the Arctic Ocean present in the LGM ICE-4G reconstruction (Fig. 2) near the Siberian coast and therefore imposed to the AGCMs as a boundary condition.

Around 90 kyr BP the reconstruction of the limits of the Eurasian ice sheet provided by Svendsen et al. (2004) indicates that the ice was spread over Norway, the Barents-Kara Seas including the Svalbard, the Franz Josef islands and Novaya and Severnaya Zemlya, and extended eastward beyond the Taimyr Peninsula, covering also the Putorana Plateau. Among the different GCMs used in this study, the forcing from ECHAM3 presents the best agreement for this period (not shown) with this synthesis.

Around the early Middle Wechselian period (60–50 kyr BP) the ice advanced over Finland, the Baltic Sea and the Kola Peninsula. In the Barents Sea, the ice sheet was more extended, while in the east, a much smaller area of Siberia is affected by the glaciation compared to the Early Wechselian period. None of the simulations performed in this study (Fig. 5) is in a perfect agreement with this reconstruction. The first point of disagreement concerns the too large expansion of the simulated ice sheet

Ice-sheet evolution during the last climatic cycle

S. Charbit et al.

Title Page

Abstract

Introduction

Conclusions

References

Tables

Figures

◀

▶

◀

▶

Back

Close

Full Screen / Esc

Printer-friendly Version

Interactive Discussion

across Eastern Siberia (CCSR1, MRI2, UGAMP and ECHAM3) while reconstructions indicate a retreat of the eastern part of the ice sheet around the Middle Wechselian period. A possible mechanism at the origin of this discrepancy could be linked to a reduction of precipitation over the eastern part when the ice sheet over the Scandinavian region became huge enough. This mechanism would be fully similar to the one suggested by Clark and Bartlein (1995) to explain the glaciation scenario of the Cordilleran-Laurentide ice complex. Therefore, in the case of the Eurasian ice sheet, this “East-West” sequence cannot be reproduced with our approach. Another cause of the presence of ice in this region lies in the fact that the ICE-4G reconstruction extends too much eastward (Fig. 2). This enhances, via the albedo effect, the advance of ice in regions located East of the Taimyr Peninsula and also favours the growth of ice in Beringia, which is also due, as previously mentioned, to the marine ice complex produced by the ICE-4G reconstruction. However, in the simulations carried out with LMD5 and GENESIS2, ice does not appear in Beringia. Therefore, in these runs, the albedo effect induced by an erroneous amount of ice in the Arctic Ocean is likely masked by another process which could be linked to the climate models themselves, such as a change in the planetary waves, which would lead in that case to warmer temperatures over Beringia. The second point of disagreement between our results and the reconstructions of the Eurasian ice sheet limits concerns the advance of ice over the Barents and the Kara Seas which is not reproduced in our simulations. This effect, which appears in all the simulations, is due to the absence of any explicit representation of the ice flow through the marine part of the ice sheets in the GREMLINS model. Although there is a parameterization which deals with the advance of ice into the sea, this advance is not rapid enough to properly reproduce the growth of the Barents-Kara Sea ice complex. The ice sheet simulated with the use of MRI2 does not penetrate southward enough, due to warm simulated summer surface air temperatures, especially to the South of the Scandinavian region, compared to those obtained with other GCMs. On the contrary, with the UGAMP model, the ice covering the Scandinavian region extends too much to the South in response to cold annual and summer

**Ice-sheet evolution
during the last
climatic cycle**

S. Charbit et al.

Title Page

Abstract

Introduction

Conclusions

References

Tables

Figures

◀

▶

◀

▶

Back

Close

Full Screen / Esc

Printer-friendly Version

Interactive Discussion

temperatures added to a high precipitation ratio in this region. The ice coverage over Scandinavia is too small with LMD5 and GENESIS2 due to warmer surface air temperatures (Figs. 1a–b). However, both these models present the best agreement with the reconstruction of the eastern ice-sheet limit. Finally, all models simulate ice over the British Isles, although they were unlikely to be glaciated during the Middle Wechselian period (Svendsen et al., 2004).

At the Last Glacial Maximum, the reconstruction of the ice limits is relatively well known. The Barents-Kara ice complex was strongly reduced and did not expand further east of Novaya Zemlya (Svendsen et al., 2004). None of the models used in the present study successfully simulate the recede of the Barents-Kara Sea ice sheet, and except for MRI2, the ice volume and the ice extent are larger compared to the Early Middle Wechselian period (Fig. 6). On the other hand, on the western side, the ice sheet advanced much more in the southwestern part, leading to a bridge between Scandinavia and the British Isles, not reproduced by GREMLINS whatever the GCM outputs used as climate forcing. However, these major drawbacks are due to the ICE-4G reconstruction itself which favours a huge ice sheet at the LGM over the Barents-Kara Seas region and, in which the junction between the European continent and the British Isles is not properly represented. Finally, as in the Middle Wechselian period, the ice coverage over Scandinavia remains insufficient in the simulations performed with LMD5 and GENESIS2.

3.2 Temporal evolution of the ice-sheet characteristics

3.2.1 The simulated Northern Hemisphere ice volumes

The evolution of the simulated ice volumes throughout the last glacial cycle is displayed in Fig. 8 for the overall Northern hemisphere and for the specific contributions of the past North American and Eurasian ice sheets. Each curve is related to one GCM forcing. The dashed line represents the Northern hemisphere ice sheet contribution to sea-level variation relative to the present-day level. This curve is obtained by removing the

Ice-sheet evolution during the last climatic cycle

S. Charbit et al.

Title Page

Abstract

Introduction

Conclusions

References

Tables

Figures

⏪

⏩

◀

▶

Back

Close

Full Screen / Esc

Printer-friendly Version

Interactive Discussion

Antarctic contribution to the sea-level reconstruction provided by Bassinot et al. (1994) and converted in ice volume equivalent, and by adding the present-day contribution of Greenland ($\sim 2.6 \times 10^{15} \text{ m}^3$) to allow a direct comparison between the simulated ice volume and the sea-level derived from experimental data. The evolution of the Antarctic ice volume throughout the last glacial-interglacial cycle is estimated with the GRISLI Antarctic ice-sheet model (Ritz et al., 2001), and the present-day Greenland contribution is estimated by averaging the results of the six PMIP-GREMLINS simulations. The conversion between sea-level and ice volume equivalent is made by assuming a constant oceanic area throughout the simulation (i.e. $\sim 3.6 \times 10^{14} \text{ m}^2$).

The evolution of the ice covered area is represented in Fig. 9. Since it is controlled by the timing of the GRIP record, the temporal evolution of both ice volumes and ice covered area is approximately the same for all the six simulations. Although, small ice caps are formed as early as 126 kyr BP (Fig. 9), they are then subjected to phases of disappearance/appearance, and the initiation of the ice sheets really takes place at around 113 kyr BP, as marked both in ice volume and ice-covered area signals (Figs. 8–9), as well as in the spatial distribution of the ice sheets (Figs. 3–4). The ice volume growth is slower than that of the ice surface. This confirms that the glacial inception is primarily characterized by a rapid extension of the ice due to the effect of the ice albedo which acts as an amplifier of the cooling mechanism and dominates the effect of accumulation which is rather responsible for the evolution of the ice thickness and hence of the ice volume. These conclusions were previously reached by Kageyama et al. (2004). However, as previously mentioned to interpret the rapid expansion of ice around 112 kyr BP (Fig. 4), the albedo effect is overestimated due to the use of LGM climate snapshots. The period following the ice-sheet nucleation is characterized by three main phases of major ice sheet growth punctuated by shorter episodes of ice retreat. The phases of ice volume increase occur between 113 and 106.2 kyr BP, 100.2 and 83.5 kyr BP and between 79.2 and 57.3 kyr BP, where a full glacial state takes place (see also Fig. 5). At 57.3 kyr BP the Northern hemisphere ice volume is 90% greater than the last glacial maximum value, located at 18.2 kyr BP, except for

Ice-sheet evolution during the last climatic cycle

S. Charbit et al.

Title Page

Abstract

Introduction

Conclusions

References

Tables

Figures

◀

▶

◀

▶

Back

Close

Full Screen / Esc

Printer-friendly Version

Interactive Discussion

ECHAM3 (83%) and MRI2 (71%). In the same way, at 57.3 kyr BP, the glaciated area is between 92 and 97% that obtained at the time of the LGM, depending on the GCM. After 18.2 kyr BP, the ice volume slightly decreases until 16.6 kyr BP. It then remains approximately stable until about 15.0 kyr BP where the main phase of the deglaciation is triggered. As described in Charbit et al. (2002), this phase is correlated with a warming event observed in the GRIP record. A slight increase of the ice volume is then observed and corresponds to the Younger-Dryas. The deglaciation of the North American ice sheet is achieved approximately between 5 and 2 kyr BP, depending on the GCM, whereas for all models the complete retreat of Fennoscandia occurs between 6 and 5 kyr BP.

However, some clear differences appear between the results of the different runs. The most striking feature is related to the amplitude of the difference between glacial and interglacial ice volume (or ice coverage area) from one GCM to the other, and more generally, between phases of growth and retreat of the ice sheet. Figure 8 clearly shows that the highest simulated ice volumes are obtained by using the UGAMP and CCSR1 outputs as climate forcing. In contrast, the use of MRI2 produces the lowest ice volume throughout the simulation except at the LGM because of the contribution of the Eurasian ice sheet. While LMD5 and GENESIS2 lead to “intermediate” ice volumes, the case of ECHAM3 is particularly interesting. In fact during the early phase of glacial inception (between 113 and 106 kyr BP), the simulated ice volume is of the same order of magnitude than those obtained with LMD5 and GENESIS2. However, after 70 kyr BP, it becomes greater (it increases by ~42% between 70 and 60 kyr BP) and reaches some values close to those obtained with CCSR1 and UGAMP. In the same way, though the ice volume simulated with the MRI2 climate remains at a low level, especially prior to 70 ka, it presents the most significant variations during the full glacial period: between 70 and 60 kyr BP, the amplitude increases by ~72% and by ~57% between 60 ka and the Last Glacial Maximum. As an example, this can be compared to the ice volume curves obtained with LMD5 and GENESIS2 which respectively increase by 14% and 10% during the same period, or with CCSR1 and

Ice-sheet evolution during the last climatic cycle

S. Charbit et al.

Title Page

Abstract

Introduction

Conclusions

References

Tables

Figures

◀

▶

◀

▶

Back

Close

Full Screen / Esc

Printer-friendly Version

Interactive Discussion

UGAMP (14 and 15% increase, respectively).

3.2.2 Links between ice volumes, climate forcing and spatial distribution

The same kind of differences also appears in the ice volume curves relative to the American or the Fennoscandian ice sheets. These differences can be interpreted in terms of climate forcing and spatial distribution of the ice sheets.

For the Laurentide ice sheet, the largest ice volumes are obtained with UGAMP and CCSR1 which provide the coldest temperatures over the Canadian region (Fig. 1): the changes in summer surface air temperature between the LGM and the present-day periods can be as high as -40°C for both models over a great part of the ice complex (Fig. 1b). The precipitation ratio between the LGM and the present-day climates simulated by UGAMP is rather small on the western and eastern parts of the ice sheet, but can reach a value as high as 2.5 in some specific locations such as the wind exposed slope of the Rocky Mountains or the southern margin of the Keewatin region (Fig. 1c). Among the GCMs used in this study, CCSR1 is the model which simulates the highest LGM/CTRL precipitation ratio over the North American ice complex. The LMD5 model provides summer temperatures as cold as those given by UGAMP and CCSR1 but the LGM precipitation ratio between the LGM and the present-day periods does not exceed 0.6. Until 65 kyr BP, the simulated ice volume obtained with ECHAM3 is below that obtained with the LMD5 climate, and becomes greater after this period (see previous section). This can be explained by the fact that, although the ECHAM3 precipitation ratio between past and present is high over the southern part of the ice complex (>1.6), the simulated summer temperatures are widely higher than the LMD5 ones (Fig. 1b). Since glacial inception is primary driven by the temperature signal the ice volume remains at a low level before the second phase of inception is reached, that is before the full glacial period. Moreover, since the ice sheet is located at low latitudes (Fig. 4) it is sensitive to any change in temperature. At 65 kyr BP an abrupt decrease in the temperature reconstructed at the surface of the ice sheet is observed in the GRIP signal (Dansgaard et al., 1993). This decrease in the temperature signal added to the

Ice-sheet evolution during the last climatic cycle

S. Charbit et al.

Title Page

Abstract

Introduction

Conclusions

References

Tables

Figures

◀

▶

◀

▶

Back

Close

Full Screen / Esc

Printer-friendly Version

Interactive Discussion

high precipitation value leads to a significant increase in the ice volume. This change in the evolution of the ice volume signal is not observed with LMD5 because the precipitation ratio is lower over the ice-sheet location. The situation is different for the comparison between GENESIS2 and LMD5: the GENESIS2 higher summer temperatures combined with higher precipitation rates lead to an ice volume fully comparable to that resulting from the LMD5 forcing climate until 95 ka, but widely below it after this period. This can be explained by the surface temperatures at the frontier between the Laurentide and the Cordilleran ice sheets which are higher than over the other regions of Canada. This prevents both ice sheets from coalescing, therefore limiting the increase of the ice volume (see Sect. 3.1). The lowest ice volume during the entire simulation is obtained by forcing GREMLINS with MRI2. The magnitude of the MRI2 precipitation ratio is between 0.4 and 0.6, but the temperatures are warmer than the LMD5 ones (not below -25°C in summer and -20°C for the annual mean).

The ice volume curves relative to the Eurasian ice sheet can be split in two groups: UGAMP, ECHAM3 and CCSR1 on one hand and LMD5, MRI2 and GENESIS2 on the other. The first group of models is characterized by low annual temperatures (i.e. the variation between past and present is -40°C over a large part of the Fennoscandian area, especially for ECHAM3 and CCSR1). The precipitation ratio is relatively small for ECHAM3 and UGAMP (0.2–0.4 North of Scandinavia), but comparable with that of MRI2 for CCSR1. Between 100 and 85 kyr BP, the ice volume simulated with ECHAM3 is greater than that obtained with UGAMP and CCSR1, due to the fact that ECHAM3 simulates the lowest summer surface air temperatures. This acts in favour of glaciation especially during the inception period. After 60 kyr BP, that is, during the full glacial period, and until about 10 kyr BP the highest volume is obtained with UGAMP which simulates a cold tongue extended far to the Northeast of Scandinavia. The second group of models is characterized by slightly higher precipitation ratios and smaller changes in summer temperatures (between -25 and -20°C for LMD5 and -20 and -15°C for MRI2 and GENESIS2), and also by the fact that the regions where the coldest temperatures are observed are less extended compared to temperature patterns

Ice-sheet evolution during the last climatic cycle

S. Charbit et al.

Title Page

Abstract

Introduction

Conclusions

References

Tables

Figures

◀

▶

◀

▶

Back

Close

Full Screen / Esc

Printer-friendly Version

Interactive Discussion

provided by the first group of models, suggesting that the evolution of the Eurasian ice sheet is rather sensitive to the temperature than to precipitation.

3.2.3 Model-model and model-data comparisons

At the LGM (i.e. 18.2 kyr BP) the Northern hemisphere simulated ice volume is between 43.6 and $73.7 \times 10^{15} \text{ m}^3$. This range can be compared to that provided by Milne et al. (2002) obtained with a radial viscoelastic ice-Earth model used to predict the sea-level change from the LGM to present in four far-field sites, and based on a revised theoretical formalism incorporating the Earth rotational effects on sea level, a time-dependent shoreline geometry and an accurate treatment of sea-level change in regions of ice retreat. By de-constructing the spatially uniform versus the spatially varying signals of sea-level change and by isolating the contributions of ice loading, ocean loading and rotational effects they concluded that the meltwater contribution dominates the far-field sea-level change signal. This meltwater component can be explicitly (Flemming et al., 1998; Yokoyama et al., 2000) or implicitly (Peltier, 1994) estimated by correcting the observations for the contribution of the glacial isostatic adjustment. Based on two contrasting interpretations of Barbados coral data, they obtained estimates of the grounded ice volume ranging from 43.5 to $51.0 \times 10^{15} \text{ m}^3$. These values are fully compatible with the ice volumes obtained with GENESIS2 ($43.6 \times 10^{15} \text{ m}^3$), MRI2 ($46.5 \times 10^{15} \text{ m}^3$) and LMD5 ($51.2 \times 10^{15} \text{ m}^3$) outputs, and suggest that ECHAM3 ($68.2 \times 10^{15} \text{ m}^3$), UGAMP ($73.7 \times 10^{15} \text{ m}^3$) and CCSR1 ($71.7 \times 10^{15} \text{ m}^3$) cannot provide a realistic climate forcing at the LGM. This is confirmed by the comparison between the sea-level curve and the simulated ice volumes.

To go a step further, it is also interesting to examine which amount of ice is distributed over the North American and the Eurasian ice sheets at the LGM (i.e. 18 kyr BP in the simulations). The contributions of both ice sheets range respectively from 36.9 to $52.9 \times 10^{15} \text{ m}^3$ ($36.6\text{--}52.4 \times 10^{15} \text{ m}^3$ at 21 kyr BP) and from 2.8 to $14.7 \times 10^{15} \text{ m}^3$ ($2.7\text{--}13.5 \times 10^{15} \text{ m}^3$ at 21 kyr BP). For the North American ice sheet, our results are neither compatible with the ICE-4G ice-sheet reconstruction (Peltier, 1994) used as bound-

Ice-sheet evolution during the last climatic cycle

S. Charbit et al.

Title Page

Abstract

Introduction

Conclusions

References

Tables

Figures

◀

▶

◀

▶

Back

Close

Full Screen / Esc

Printer-friendly Version

Interactive Discussion

ary condition for the AGCM LGM runs, nor with the more recent ICE-5G topography (Peltier, 2004). Both reconstructions provide ice volume values which are well below our lower limit ($24.5 \times 10^{15} \text{ m}^3$ and $34.3 \times 10^{15} \text{ m}^3$ for ICE-4G and ICE-5G, respectively). The reconstructed Fennoscandian ice volume is $8.7 \times 10^{15} \text{ m}^3$ for ICE-4G and $9 \times 10^{15} \text{ m}^3$ for ICE-5G. These reconstructions lie in the range of our set of simulations. However, compared to these reconstructions, the first group of models ($2.8 \times 10^{15} \text{ m}^3$ – $5.6 \times 10^{15} \text{ m}^3$) underestimates the ice volume, while the ice volumes obtained with the second group ($10.5 \times 10^{15} \text{ m}^3$ – $14.7 \times 10^{15} \text{ m}^3$) are overestimated.

To quantify the uncertainties associated with glaciological reconstructions of the North American ice sheet, Marshall et al. (2002) carried out numerous experiments with a 3-D thermo-mechanical model prescribing different climatic conditions and different glaciological and isostatic treatments. Considering only the simulations which gave a reasonable areal extent of the ice sheet, this provided values ranging from 28.5 to $38.9 \times 10^{15} \text{ m}^3$, only in accordance with the modeling results obtained with GENESIS2 ($36.9 \times 10^{15} \text{ m}^3$) and MRI2 ($37.2 \times 10^{15} \text{ m}^3$). Using an ice-sheet model, forced by global sea-level and solar insolation changes, Siegert et al. (2001, 1999) modeled the Eurasian ice sheet through the Late Weichselian period. They adjusted their “model’s climate forcing function” to produce a minimum and a maximum ice sheet reconstruction compatible with geological and oceanographic datasets. The simulated LGM ice volumes are respectively at around 5 and $8 \times 10^{15} \text{ m}^3$, in agreement with what we find with LMD5 only ($5.4 \times 10^{15} \text{ m}^3$): the results obtained with GENESIS2 and MRI2 are well below the minimum ice volume, whereas UGAMP ($14.7 \times 10^{15} \text{ m}^3$), CCSR1 ($10.5 \times 10^{15} \text{ m}^3$) and ECHAM3 ($11.9 \times 10^{15} \text{ m}^3$) provide values which widely exceed those obtained with the maximum model.

The comparison between our results and other modeling studies or sea-level data suggests that most of the simulations presented in this study overestimate the ice volume throughout the last glacial cycle. This can be due to sub-grid processes, not represented in the ice-sheet model, which may have had accelerated the ice flow, such as the flow of several large glaciers which accelerates the overall ice discharge,

Ice-sheet evolution during the last climatic cycle

S. Charbit et al.

Title Page

Abstract

Introduction

Conclusions

References

Tables

Figures

◀

▶

◀

▶

Back

Close

Full Screen / Esc

Printer-friendly Version

Interactive Discussion

as it has been demonstrated with recent measurements for the Greenland ice sheet (Dowdeswell, 2006; Rignot and Kanagaratnam, 2006).

4 Conclusions

The climatic outputs from six PMIP-AGCMs have been used to force a 3-D thermo-mechanical ice-sheet model. This study reveals some great differences from one simulation to the other related both to the simulated temporal evolution of the ice volumes and ice-covered area and to the shape and spatial distribution of the ice sheets. The differences related to the evolution of the ice volumes can be partly directly interpreted in terms of climate forcing. Moreover, these differences also depend on the location of primary ice sheets which is, by the way, directly influenced by the climate itself. As an example, ice masses located at low latitudes in the early phase of glaciation are more sensitive to a temperature variation than a higher latitude ice sheet.

The comparison of our simulated ice sheets with geological and sea-level data highlights the importance of some major ice-climate feedbacks and raises the question of to which extent this kind of approach enables to test the ability of GCMs to simulate a climate leading to ice sheets compatible with available geological and geomorphological reconstructions. Actually, none of the simulations presented in this study is able to reproduce ice sheets in full agreement with observations. The main points of disagreement concern:

1. The location of sites of primary inception which can directly be attributed to the climate forcing. For the Eurasian ice sheet, the Taimyr Peninsula is reasonably glaciated. However, observations indicate that the regions of ice-sheet inception in North America were those bordering the eastern coast (Baffin Island and Quebec-Labrador sector) as well as the uplands of Northeastern Keewatin, which is not perfectly reproduced in the simulations.

2. The chronology of the simulated glaciation of the Rocky Mountains region which

CPD

2, 879–921, 2006

Ice-sheet evolution during the last climatic cycle

S. Charbit et al.

Title Page

Abstract

Introduction

Conclusions

References

Tables

Figures

⏪

⏩

◀

▶

Back

Close

Full Screen / Esc

Printer-friendly Version

Interactive Discussion

EGU

Ice-sheet evolution during the last climatic cycle

S. Charbit et al.

Title Page

Abstract

Introduction

Conclusions

References

Tables

Figures

⏪

⏩

◀

▶

Back

Close

Full Screen / Esc

Printer-friendly Version

Interactive Discussion

starts to be glaciated as early as 113 kyr BP, while according to data, the Cordilleran ice sheet does not appear to have developed before 75 kyr BP when the Laurentide ice sheet was high enough to induce a displacement of the jet stream. This sequence of events cannot be properly reproduced with our approach due to the absence of any ice-sheet feedback on the atmospheric circulation. Moreover, the use of LGM climate snapshots in the climate forcing overestimates the albedo effect throughout the simulation in regions covered by snow at the LGM, and, hence, accelerates the glaciation process. Subsequently, the advance of ice in Alaska is probably favored, via the artefact albedo effect, by the early glaciation of the Cordilleran ice sheet.

3. The presence of ice in Siberia, which is not due to the absence of any representation of the feedback processes of the ice sheets on climate, since Siberia has remained unglaciated throughout the last glacial-interglacial cycle. In fact, the glaciation of the Siberian region is probably linked to the cold temperatures simulated by the climate models in response to the erroneous amount of ice provided by the LGM ICE-4G reconstruction (Peltier, 1994).
4. The too large eastward expansion of the Eurasian ice sheet around the Middle Wechselian period due partly to the ICE-4G reconstruction and to the fact that our approach is not able to reproduce a reduction of precipitation in the eastern part, concomitant with the growth of ice over the Scandinavian region.
5. The insufficient penetration of the Barents-Kara sea ice sheet into the sea, which due to the absence in the GREMLINS model of any explicit representation of the ice flow through the marine part of the ice sheets.
6. The extent of the Scandinavian ice sheet: very few models succeed in simulating a reasonable amount ice over Fennoscandia (except the simulations carried out with ECHAM3 and UGAMP). This can be analyzed in terms of mean summer temperature and of a deficit of precipitation in the north leading to an insufficient

Ice-sheet evolution during the last climatic cycle

S. Charbit et al.

Title Page

Abstract

Introduction

Conclusions

References

Tables

Figures

⏪

⏩

◀

▶

Back

Close

Full Screen / Esc

Printer-friendly Version

Interactive Discussion

northward expansion of the ice sheet. This raises the question of the sensitivity of the ice-sheet model to the climate forcing.

This study clearly demonstrates the great sensitivity of the ice sheets to the climate forcing. The great variability in the simulated climates used in the present study induces large differences in simulated ice sheets. Moreover, owing to the fact that some ice-climate feedbacks cannot be accounted for with this kind of approach, the magnitude of the climatic impacts on the ice sheet evolution are likely to be poorly estimated.

The deviations of our simulations from geological data are partly due to an over-estimation of the albedo effect in the climate simulations due to shortcomings in the ICE-4G reconstruction. Therefore, it should be interesting to carry out the same kind of experiments with models used within the framework of the second phase of the PMIP project (PMIP2). On one hand these GCMs are coupled ocean-atmosphere models, in which the SSTs (Kageyama et al., 2006) appear to be more realistic than the CLIMAP ones used in PMIP1; on the other hand the LGM runs are performed with the up-to-date ICE-5G reconstruction, which is a revised version of the ICE-4G model. This would allow the impact of the initial conditions to be tested. Moreover, these simulations will be performed with a new version of the Northern hemisphere ice sheet model which will include an explicit representation of the ice flow through ice shelves. Hence, by reducing the number of shortcomings in this kind of approach, it will be easier to attribute a kind of evaluation criteria of the PMIP2 model results which will appear in the next IPCC report.

Acknowledgements. We acknowledge all PMIP members. We also benefited of fruitful discussions with scientists participating to the MOTIF project. Thanks are also due to J.-Y. Peter-schmitt for technical support and for providing PMIP database and PMIP and MOTIF websites (<http://www-lsce.cea.fr/pmip>, <http://www-lsce.cea.fr/motif>).

References

- Adler, R. F., Susskind, J., Huffman, G. J., Bolvin, D., Nelkin, E., Chang, A., Ferraro, R., Gruber, A., Xie, P.-P., Janowiak, J., Rudolf, B., Schneider, U., Curtis, S., and Arkin, P.: The Version-2 Global Precipitation Climatology Project (GPCP) Monthly Precipitation Analysis (1979–Present), *J. Hydrometeorol.*, 4(6), 1147–1167, 2003.
- Alexander, R. C. and Mobley, R. L.: Monthly average sea surface temperatures and ice pack limits on a 1 global grid, *Mon. Wea. Rev.*, 104, 143–148, 1976.
- Andersen, K. K., Azuma, N., Barnola, J.-M., Bigler, M., Biscaye, P., Caillon, N., Chappellaz, J., Clausen, H. B., Dahl-Jensen, D., Fischer, H., et al.: High-resolution record of Northern Hemisphere climate extending into the last interglacial period, *Nature*, 431, 147–151, 2004.
- Andrews, J. T. and Barry, R. G.: Glacial inception and disintegration during the last glaciation, *Ann. Rev. Earth Planet. Sci.*, 6, 205–228, 1978.
- Bamber, J. L., Layberry, R. L., and Gogenini, S. P.: A new ice thickness and bed data set for the Greenland ice sheet. 1. Measurement, data reduction and errors., *J. Geophys. Res.*, 106(D24), 33 773–33 780, 2001.
- Bard, E., Hamelin, B., and Fairbanks, R. B.: U-Th ages obtained by mass spectrometry in corals from Barbados: sea level during the past 130 000 years, *Nature*, 346, 456–458, 1990.
- Bard, E., Jouannic, C., Hamelin, B., Pirazzoli, P., Arnold, M., Faure, G., Sumosusastro, P., and Syaefudin: Pleistocene sea levels and tectonic uplift based on dating of corals from Sumba Island, Indonesia, *Geophys. Res. Lett.*, 23(12), 1473–1476, 1996.
- Bard, E., Rostek, F., and Ménot-Combes, G.: A better radiocarbon clock, *Science*, 303, 178–179, 2004.
- Bassinot, F., Labeyrie, L. D., Vincent, E., Quidelleur, X., Shackleton, N. J., and Lancelot, Y.: The astronomical theory of climate and the age of the Brunhes-Matuyama magnetic reversal, *Earth Planet. Sci. Lett.*, 126, 91–108, 1994.
- Berger, A.: Long-term variations of daily insolation and quaternary climatic changes, *J. Atmos. Sci.*, 35, 2362–2367, 1978.
- Bintanja, R., van de Wal, R. S. W., and Oerlemans, J.: Global ice volume variations through the last glacial cycle simulated by a 3-D ice dynamical model, *Quat. Int.*, 95–96, 11–23, 2002.
- Bond, G., Broecker, W., Johnsen, S., McManus, J., Labeyrie, L., Jouzel, J., and Bonani, G.: Correlations between climate records from North Atlantic sediments and Greenland ice, *Nature*, 365, 143–147, 1993.

CPD

2, 879–921, 2006

Ice-sheet evolution during the last climatic cycle

S. Charbit et al.

Title Page

Abstract

Introduction

Conclusions

References

Tables

Figures

◀

▶

◀

▶

Back

Close

Full Screen / Esc

Printer-friendly Version

Interactive Discussion

EGU

Charbit, S., Ritz, C., and Ramstein, G.: Simulations of Northern Hemisphere ice-sheet retreat: sensitivity to physical mechanisms involved during the Last Deglaciation., *Quat. Sci. Rev.*, 21, 243–265, 2002.

Clague, J. J. and James, T. S.: History and isostatic effects of the last ice sheet in southern British Columbia, *Quat. Sci. Rev.*, 21, 71–87, 2002.

Clark, P. U. and Bartlein, P. J.: Correlation of Late Pleistocene glaciation in the western United States with North Atlantic Heinrich events, *Geology*, 23(6), 483–486, 1995.

Clark, P. U., Clague, J. J., Curry, B. B., Dreimanis, A., Hicock, S. R., Miller, G. H., Berger, G. W., Eyles, N., Lamothe, M., Miller, B. B., Mott, R. J., Oldale, R. N., Stea, R. R., Szabo, J. P., Thorleifson, L. H., and Vincent, J.-S.: Initiation and development of the Laurentide and Cordilleran ice sheets following the last interglaciation, *Quat. Sci. Rev.*, 12, 79–114, 1993.

CLIMAP: Seasonal reconstruction of the Earth surface at the Last Glacial Maximum, Geological Society of America, Boulder, Colorado, 1981.

Dansgaard, W., Johnsen, S. J., Clausen, H. B., Dahl-Jensen, D., Gundestrup, N. S., Hammer, C. U., Hvidberg, C. S., Steffensen, J. P., Sveinbjörnsdottir, A. E., Jouzel, J., and Bond, G.: Evidence for general instability of past climate from a 250-kyr ice-core record, *Nature*, 364, 218–220, 1993.

Deblonde, G. and Peltier, W. R.: Simulations of continental ice sheet growth over the last glacial-interglacial cycle: experiments with a one-level seasonal energy balance model including realistic geography, *J. Geophys. Res.*, 96(D5), 9189–9215, 1991.

Deblonde, G., Peltier, W. R., and Hyde, W. T.: Simulations of continental ice sheet growth over the last glacial-interglacial cycle: experiments with a one-level seasonal energy balance model including seasonal ice albedo feedback, *Palaeogeography, Palaeoclimatology, Palaeoecology (Global and Planetary Change Section)*, 98, 37–55, 1992.

Dowdeswell, J. A.: The Greenland ice sheet and global sea-level rise, *Science*, 311, 963–964, 2006.

Dyke, A. S., Andrews, J. T., Clark, P. U., England, J. H., Miller, G. H., Shaw, J., and Veillette, J. J.: The Laurentide and Innuitian ice sheets during the Last Glacial Maximum, *Quat. Sci. Rev.*, 21, 9–31, 2002.

Dyke, A. S. and Prest, V. K.: Late Wisconsinian and Holocene retreat of the Laurentide ice sheet, in: Geological Survey of Canada, Ottawa, Ontario, Map 1702A, scale: 1:500 000, 1987.

Edwards, M. O.: Global gridded elevation and bathymetry (ETOPO5) digital raster data on a

Ice-sheet evolution during the last climatic cycle

S. Charbit et al.

Title Page

Abstract

Introduction

Conclusions

References

Tables

Figures

◀

▶

◀

▶

Back

Close

Full Screen / Esc

Printer-friendly Version

Interactive Discussion

**Ice-sheet evolution
during the last
climatic cycle**S. Charbit et al.

[Title Page](#)[Abstract](#)[Introduction](#)[Conclusions](#)[References](#)[Tables](#)[Figures](#)[◀](#)[▶](#)[◀](#)[▶](#)[Back](#)[Close](#)[Full Screen / Esc](#)[Printer-friendly Version](#)[Interactive Discussion](#)

5-minute geographic (lat × lon) 2160×4320 (centroid-registered) grid, National Oceanic and Atmospheric Administration, Boulder, Colorado, 1989.

Fairbanks, R. G.: A glacio-eustatic sea-level record: influence of glacial melting rates on the Younger Dryas event and deep ocean circulation, *Nature*, 342, 637–641, 1989.

5 Gallée, H., van Ypersele, J. P., Fichefet, T., Tricot, C., and Berger, A.: Simulation of the last glacial cycle by a coupled, sectorially averaged climate-ice-sheet model 2. Response to insolation and CO₂ variations, *J. Geophys. Res.*, 97(D14), 15713–15740, 1992.

Greve, R., Weis, M., and Hutter, K.: Palaeoclimatic evolution and present conditions of the Greenland ice sheet in the vicinity of summit: an approach by large-scale modelling, *Paleoclimates*, 2(2–3), 133–161, 1998.

10 Huybrechts, P.: Sea-level changes at the LGM from ice-dynamic reconstructions of the Greenland and Antarctic ice sheets during the glacial cycles, *Quat. Sci. Rev.*, 21, 203–231, 2002.

Johnsen, S. J., Dahl-Jensen, D., Dansgaard, D., and Gundestrup, N.: Greenland paleotemperatures derived from GRIP bore hole temperature and ice core isotope profiles, *Tellus*, 47(B), 624–269, 1995.

15 Joseph, D.: Navy 10' global elevation values, National Center for Atmospheric Research, Boulder, Colorado, 3 pp, 1980.

Joussaume, S. and Taylor, K.: Status of the Paleoclimate Modelling Intercomparison Project (PMIP), in: First International AMIP Conference, edited by: Gates, W. L., Proceedings of the first international AMIP Conference, *World Meteorol. Organ.*, Geneva, pp 425–430, 1995.

20 Kageyama, M., Charbit, S., Ritz, C., Khodri, M., and Ramstein, G.: Quantifying ice-sheet feedbacks during the last glacial inception, *Geophys. Res. Lett.*, 31(L24203), doi:10.1029/2004GLO21339, 2004.

Kageyama, M., Laine, A., Abe-Ouchi, A., Braconnot, P., Cortijo, E., Crucifix, M., de Vernal, A., Guiot, J., Hewitt, C. D., Kitoh, A., et al.: Last Glacial Maximum temperatures over the North Atlantic, Europe and Western Siberia: a comparison between PMIP models, MARGO sea-surface temperatures and pollen-based reconstructions, *Quat. Sci. Rev.*, 25(17–18), 2082–2102, 2006.

25 Kineman, J.: FNOC/NCAR Global elevation, Terrain, and Surface Characteristics, Digital Dataset, 28 MB, 1985.

30 Kleman, J., Fastook, J., and Stroeven, A. P.: Geologically and geomorphologically constrained numerical model of Laurentide ice sheet inception and build-up, *Quat. Int.*, 95–96, 87–98, 2002.

**Ice-sheet evolution
during the last
climatic cycle**S. Charbit et al.

[Title Page](#)[Abstract](#)[Introduction](#)[Conclusions](#)[References](#)[Tables](#)[Figures](#)[◀](#)[▶](#)[◀](#)[▶](#)[Back](#)[Close](#)[Full Screen / Esc](#)[Printer-friendly Version](#)[Interactive Discussion](#)

- Lambeck, K.: Constraints on the Late Weichselian ice sheet over the Barents Sea from observations of raised shorelines, *Quat. Sci. Rev.*, 14, 1–16, 1995.
- Lambeck, K. and Chappell, J.: Sea level change through the last glacial cycle, *Science*, 292, 679–686, 2001.
- 5 Lambeck, K., Yokoyama, Y., Johnston, P., and Purcell, A.: Global ice volumes at the Last Glacial Maximum and early Lateglacial, *Earth Planet. Sci. Lett.*, 181, 513–527, 2000.
- Lambeck, K., Yokoyama, Y., and Purcell, T.: Into and out of the last glacial maximum: sea-level change during oxygen isotopes stages 3 and 2, *Quat. Sci. Rev.*, 21, 343–360, 2002.
- Mann, D. H. and Hamilton, T. H.: Late Pleistocene and Holocene paleoenvironments of the
10 North Pacific Coast, *Quat. Sci. Rev.*, 14, 449–471, 1995.
- Marshall, S. J.: Modelled nucleation centres of the Pleistocene ice sheets from an ice sheet model with sugrid topographic and glaciologic parameterizations, *Quat. Int.*, 95–96, 125–137, 2002.
- Marshall, S. J., James, T. S., and Clarke, G. K. C.: North American ice sheet reconstructions at
15 the Last Glacial Maximum, *Quat. Sci. Rev.*, 21, 175–192, 2002.
- Marshall, S. J., Tarasov, L., Clarke, G. K. C., and Peltier, W. R.: Glaciological reconstruction of the Laurentide Ice Sheet: physical processes and modelling challenges, *Can. J. Earth Sci.*, 37, 769–793, 2000.
- Marsiat, I.: Simulation of the Northern Hemisphere continental ice sheets over the last glacial
20 interglacial cycle: experiments with a latitude-longitude vertically integrated ice sheet model coupled to a zonally averaged climate model, *Paleoclimates*, 1(1), 59–98, 1994.
- Milne, G. A., Mitrovica, J. X., and Schrag, D. P.: Estimating past continental ice volume from sea-level data, *Quat. Sci. Rev.*, 21, 361–376, 2002.
- New, M., Hulme, M., and Jones, P.: Representing twentieth-century space-time climate variability. Part 1: Development of a 1961–90 mean monthly terrestrial climatology., *J. Climate*,
25 12, 829–856, 1999.
- Ohmura, A. and Reeh, N.: New precipitation and accumulation maps for Greenland, *J. Glaciol.*, 37, 140–148, 1991.
- Peltier, W. R.: Ice age paleotopography, *Science*, 265, 195–201, 1994.
- 30 Peltier, W. R.: Global glacial isostasy and the surface of the ice-age Earth: the ICE-5G (VM2) model and GRACE, *Ann. Rev. Earth Planet. Sci.*, 32, 111–149, 2004.
- Peltier, W. R. and Marshall, S.: Coupled energy-balance/ice-sheet model simulations of the glacial cycle: A possible connection between terminations and terrigenous dust, *J. Geo-*

**Ice-sheet evolution
during the last
climatic cycle**S. Charbit et al.

- phys. Res. Lett., 100(D7), 14 269–14 289, 1995.
- Pollard, D. and Groups, P. P.: Comparisons of ice-sheet surface mass budgets from Paleoclimate Modeling Intercomparison Project (PMIP) simulations, *Global and Planetary Change*, 24, 79–106, 2000.
- 5 Raynaud, D., Jouzel, J., Barnola, J.-M., Chappelaz, J., Delmas, R. J., and Lorius, C.: The ice record of greenhouse gases, *Science*, 259, 926–934, 1993.
- Reeh, N.: Parameterization of melt rate and surface temperature on the Greenland ice sheet, *Polarforschung*, 59, 113–128, 1991.
- Reimer, P. J., Baillie, M. G. L., Bard, E., Bayliss, A., Warren Beck, J., Bertrand, C. J. H.,
10 Blackwell, P. G., Buck, C. E., Burr, G. S., Cutler, K. B., et al.: IntCal04 Terrestrial radiocarbon age calibration 0–26 kyr BP, *Radiocarbon*, 46(3), 1029–1058, 2004.
- Reynolds, R. W.: A real-time global sea-surface temperature analysis, *J. Climate*, 1, 75–86, 1988.
- Rignot, E. and Kanagaratnam, P.: Changes in the velocity structure of the Greenland ice sheet,
15 *Science*, 311, 986–990, 2006.
- Ritz, C., Fabre, A., and Letréguilly, A.: Sensitivity of a Greenland ice sheet model to ice flow and ablation parameters: consequences for the evolution through the last climatic cycle, *Clim. Dyn.*, 13, 11–24, 1997.
- Ritz, C., Rommelaere, V., and Dumas, C.: Modeling the Antarctic ice sheet evolution of the
20 last 420 000 years: implication for altitude changes in the Vostok region, *J. Geophys. Res.*, 106(D23), 31 943–31 964, 2001.
- Serreze, M. C. and Hurst, C. R.: Representation of mean Arctic precipitation from NCEP-NCAR and ERA reanalyses., *J. Climate*, 13, 182–201, 2001.
- Shea, D. J., Trenberth, K. E., and Reynolds, R. W.: A global monthly sea-surface temperature
25 climatology, NCAR technical note, NCAR/TN-345, 167 pp, 1990.
- Siegert, M. J., Dowdeswell, J. A., Hald, M., and Svendsen, J. I.: Modelling the Eurasian ice sheet through a full (Wechselian) glacial cycle, *Global and Planetary Change*, 31, 367–385, 2001.
- Siegert, M. J., Dowdeswell, J. A., and Melles, M.: Late Wechselian Glaciation of the Russian
30 high Arctic, *Quat. Res.*, 52, 273–285, 1999.
- Svendsen, J. I., Alexanderson, H., Astakhov, V. I., Demidov, I., Dowdeswell, J., Funder, S., Gataullin, V., Henriksen, M., Hjort, C., Houmark-Nielsen, M., et al.: Late Quaternary ice sheet history of Northern Eurasia, *Quat. Sci. Rev.*, 23, 1229–1271, 2004.

[Title Page](#)[Abstract](#)[Introduction](#)[Conclusions](#)[References](#)[Tables](#)[Figures](#)[◀](#)[▶](#)[◀](#)[▶](#)[Back](#)[Close](#)[Full Screen / Esc](#)[Printer-friendly Version](#)[Interactive Discussion](#)

Tarasov, L. and Peltier, W. R.: Terminating the 100 kyr ice age cycle, *J. Geophys. Res.*, 102(D18), 21 665–21 693, 1997.

Tarasov, L. and Peltier, W. R.: Impact of thermomechanical ice sheet coupling of the 100 kyr ice age cycle, *J. Geophys. Res.*, 104(D8), 9517–9545, 1999.

5 Tarasov, L. and Peltier, W. R.: A geophysically constrained large ensemble analysis of the deglacial history of the North American ice sheet complex, *Quat. Sci. Rev.*, 23, 359–388, 2004.

10 Waelbroeck, C., Labeyrie, L., Michel, E., Duplessy, J. C., McManus, J. F., Lambeck, K., Balbon, E., and Labracherie, M.: Sea-level and deep water temperature changes derived from benthic foraminifera isotopic records, *Quat. Sci. Rev.*, 21, 295–305, 2002.

Yokoyama, Y., Lambeck, K., De Dekker, P., Johnston, P., and Fifield, L. K.: Timing of the Last Glacial Maximum from observed sea-level minima, *Nature*, 406, 713–716, 2000.

15 Zweck, C. and Huybrechts, P.: Modeling of the northern hemisphere ice sheets during the last glacial cycle and glaciological sensitivity, *J. Geophys. Res.*, 110, D07103, doi:10.1029/2004JD005489, 2005.

CPD

2, 879–921, 2006

Ice-sheet evolution during the last climatic cycle

S. Charbit et al.

Title Page

Abstract

Introduction

Conclusions

References

Tables

Figures

◀

▶

◀

▶

Back

Close

Full Screen / Esc

Printer-friendly Version

Interactive Discussion

EGU

Table 1. Characteristics of the AGCM runs.

Models	Resolution (long × lat × vert.)	SST (21 ka)	SST (0 ka)	Sea ice (21 ka)	Sea ice (0 ka)	Orography (21 ka)	Orography (0 ka)
UGAMP	128×64×19	CLIMAP 21 ka	AIMob.76	CLIMAP 21 ka	AIMob.76	PMIP	AMIP
ECHAM3	128×64×19	PMIP	AMIP	CLIMAP 21 ka	AMIP	PMIP	AMIP
GENESIS2	96×48×18	CLIMAP 21 ka	Shea.90	CLIMAP 21 ka	Shea.90	PMIP	US Navy-FNOC.85
MRI2	72×46×15	PMIP	AMIP	CLIMAP 21 ka	AMIP	PMIP	AMIP
LMD5	64×50×11	PMIP	AMIP	CLIMAP 21 ka	AMIP	PMIP	AMIP
CCSR1	64×32×20	PMIP	AMIP	CLIMAP 21 ka	AMIP	PMIP	ETOPO5.85

Column 2 : Horizontal resolution and number of vertical levels for each model (column 2);
 Columns 3–8 indicate how the boundary conditions (SSTs, sea-ice cover and orography) have
 been taken into account for each GCM run:

Column 3: [PMIP] = CLIMAP 21 kyr BP – CLIMAP 0 ka + SSTs data used for the control run
 (see column 4)

Column 4: [AMIP] = Reynold’s data (1979–1988) – 10 years mean (Reynolds, 1988)

AIMob_76 = data from Alexander and Mobley (1976)

Shea_90 = data from Shea et al. (1990)

Column 5: data from (CLIMAP, 1981)

Column 6: [AMIP] = data from US Navy and National oceanic an Atmospheric Administration

AIMob_76 = data from Alexander and Mobley (1976))

Column 7: [PMIP] = ICE-4G (21 ka) – ICE-4G (0 ka) + orography used for the control run (see
 column 8)

Column 8: [AMIP] = U.S. Navy 10′ × 10′ dataset (Joseph, 1980)

US navy-FNOC_85: area-averaged dataset over each atmospheric grid box (Kineman, 1985)

ETOPO5_85 = obtained at a resolution of 5′ × 5′ (Edwards, 1989)

Ice-sheet evolution during the last climatic cycle

S. Charbit et al.

Title Page

Abstract

Introduction

Conclusions

References

Tables

Figures

◀

▶

◀

▶

Back

Close

Full Screen / Esc

Printer-friendly Version

Interactive Discussion

Ice-sheet evolution during the last climatic cycle

S. Charbit et al.

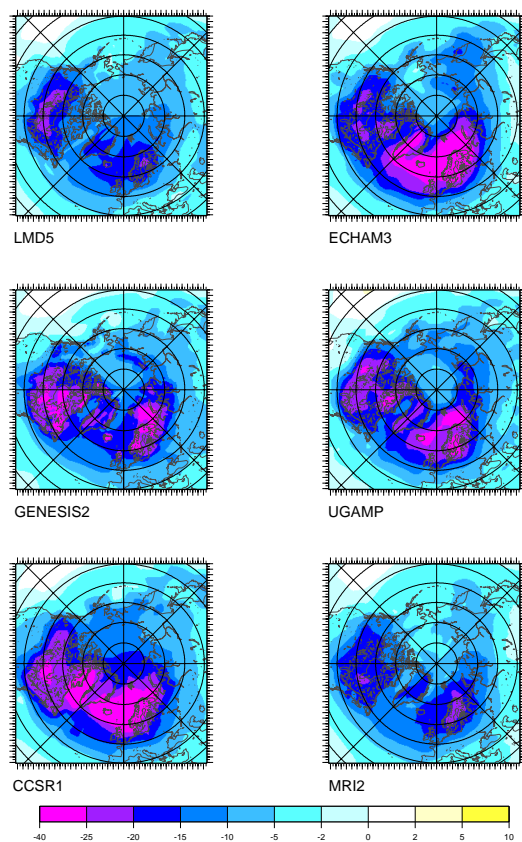


Fig. 1. (a) Mean annual surface air temperature differences between past (21 kyr BP) and present simulated by each of the atmospheric general circulation model and interpolated on the ice-sheet model grid.

Title Page

Abstract

Introduction

Conclusions

References

Tables

Figures

◀

▶

◀

▶

Back

Close

Full Screen / Esc

Printer-friendly Version

Interactive Discussion

Ice-sheet evolution during the last climatic cycle

S. Charbit et al.

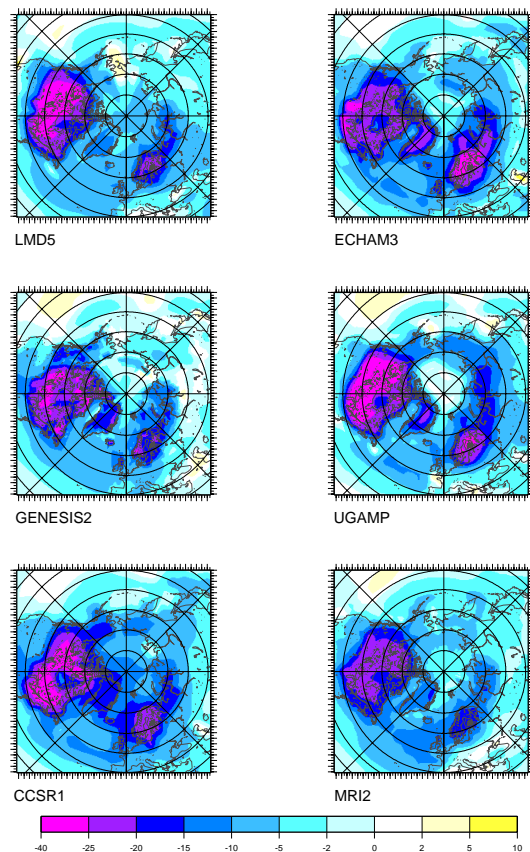


Fig. 1. (b) Same as Fig. 1a, but for the mean summer surface air temperature.

Title Page

Abstract

Introduction

Conclusions

References

Tables

Figures

◀

▶

◀

▶

Back

Close

Full Screen / Esc

Printer-friendly Version

Interactive Discussion

**Ice-sheet evolution
during the last
climatic cycle**

S. Charbit et al.

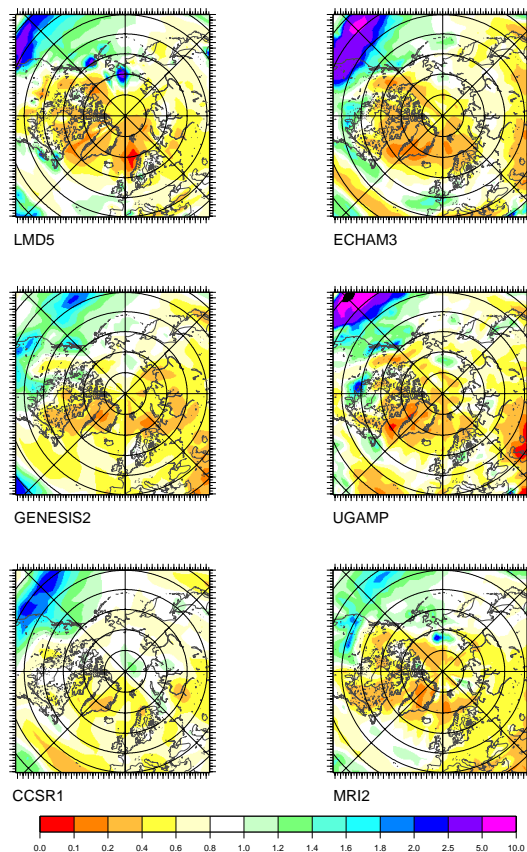


Fig. 1. (c) Ratio of mean annual precipitation (past/present) simulated by each of the atmospheric general circulation model and interpolated on the ice-sheet model grid.

[Title Page](#)[Abstract](#)[Introduction](#)[Conclusions](#)[References](#)[Tables](#)[Figures](#)[◀](#)[▶](#)[◀](#)[▶](#)[Back](#)[Close](#)[Full Screen / Esc](#)[Printer-friendly Version](#)[Interactive Discussion](#)

Ice-sheet evolution during the last climatic cycle

S. Charbit et al.

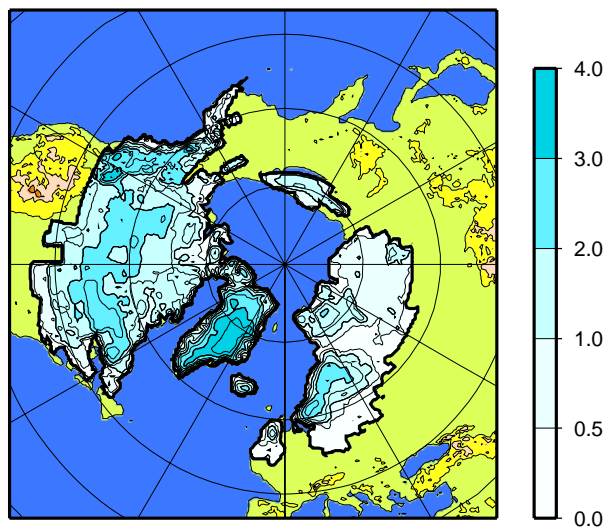


Fig. 2. Extension and ice thickness (in km) of the Northern hemisphere ice sheets predicted by the ICE-4G model (Peltier, 1994).

Title Page

Abstract

Introduction

Conclusions

References

Tables

Figures

◀

▶

◀

▶

Back

Close

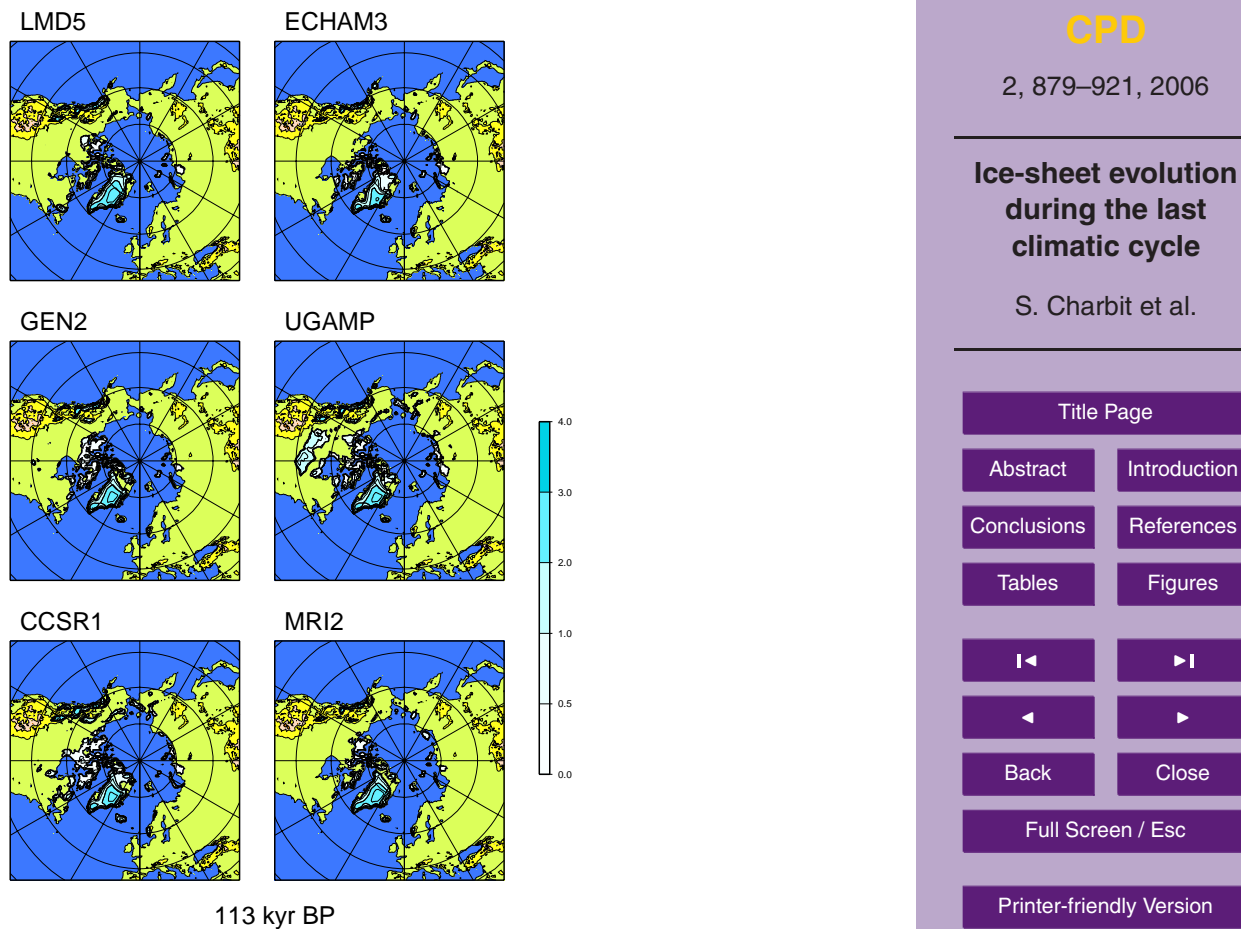
Full Screen / Esc

Printer-friendly Version

Interactive Discussion

**Ice-sheet evolution
during the last
climatic cycle**

S. Charbit et al.



113 kyr BP

Fig. 3. Spatial distribution and ice thickness (in km) of the simulated ice sheets at 113 kyr BP which corresponds to the early phase of glaciation.

Title Page

Abstract

Introduction

Conclusions

References

Tables

Figures

◀

▶

◀

▶

Back

Close

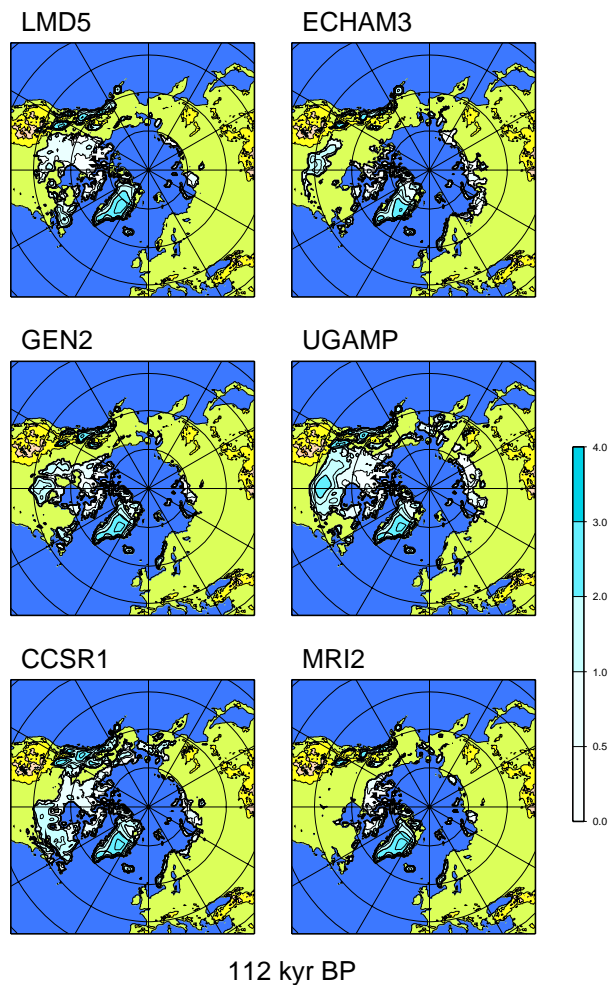
Full Screen / Esc

Printer-friendly Version

Interactive Discussion

**Ice-sheet evolution
during the last
climatic cycle**

S. Charbit et al.



112 kyr BP

Fig. 4. Same as Fig. 3 for the 112 kyr BP period.

Title Page

Abstract

Introduction

Conclusions

References

Tables

Figures

◀

▶

◀

▶

Back

Close

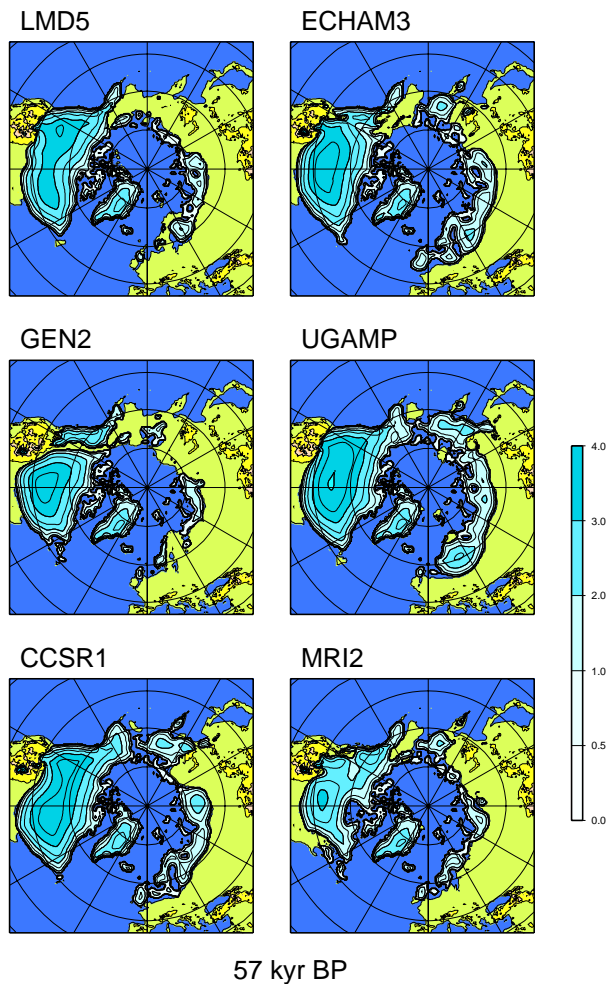
Full Screen / Esc

Printer-friendly Version

Interactive Discussion

**Ice-sheet evolution
during the last
climatic cycle**

S. Charbit et al.



57 kyr BP

Fig. 5. Same as Fig. 3 for the 57 kyr BP period which corresponds to a full glacial state.

Title Page

Abstract

Introduction

Conclusions

References

Tables

Figures

◀

▶

◀

▶

Back

Close

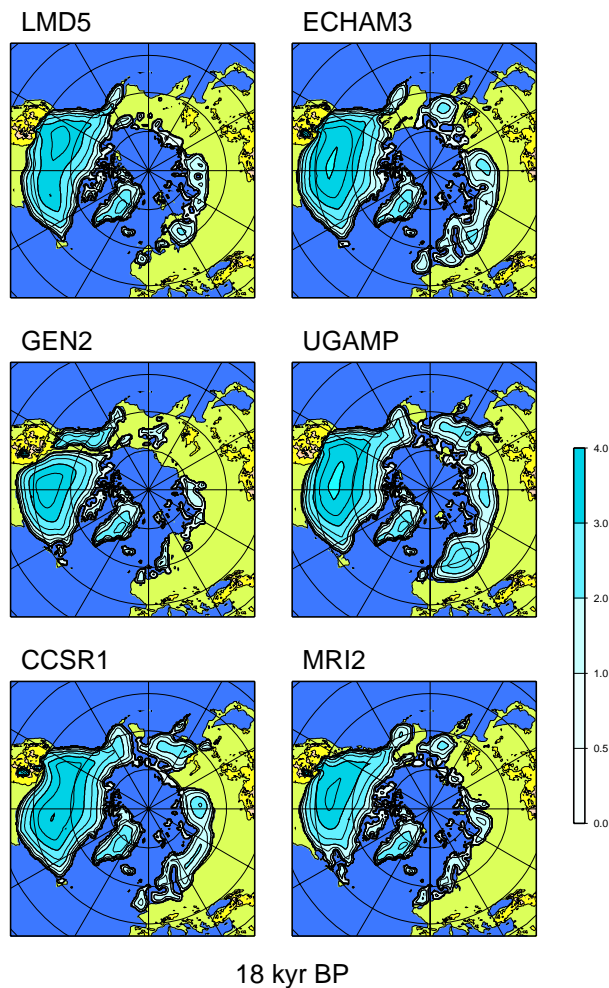
Full Screen / Esc

Printer-friendly Version

Interactive Discussion

**Ice-sheet evolution
during the last
climatic cycle**

S. Charbit et al.



18 kyr BP

Fig. 6. Same as Fig. 3 for the 18 kyr BP period which corresponds to the maximum simulated ice volume.

Title Page

Abstract

Introduction

Conclusions

References

Tables

Figures

◀

▶

◀

▶

Back

Close

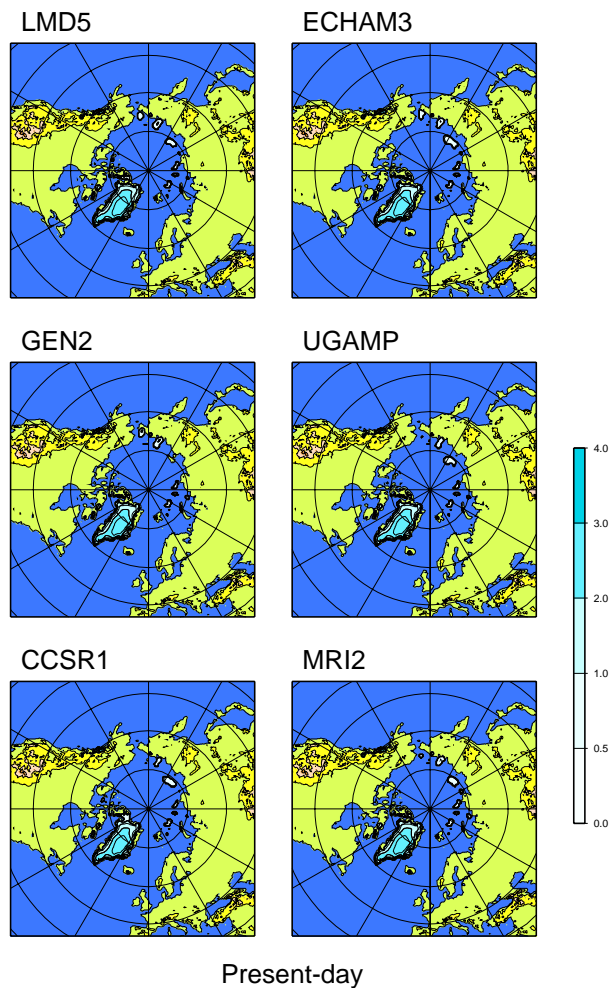
Full Screen / Esc

Printer-friendly Version

Interactive Discussion

**Ice-sheet evolution
during the last
climatic cycle**

S. Charbit et al.

**Fig. 7.** Same as Fig. 3 for the present-day period.

Title Page

Abstract

Introduction

Conclusions

References

Tables

Figures

◀

▶

◀

▶

Back

Close

Full Screen / Esc

Printer-friendly Version

Interactive Discussion

Ice-sheet evolution during the last climatic cycle

S. Charbit et al.

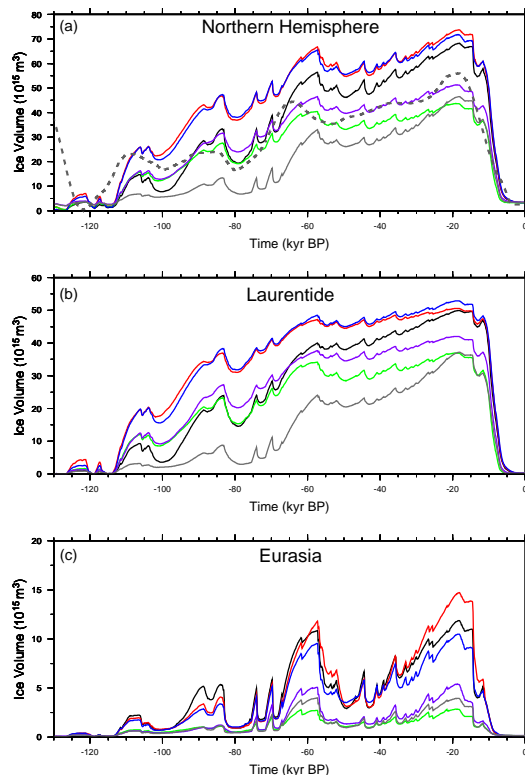


Fig. 8. Temporal evolution of the simulated ice volumes for the Northern hemisphere (a) and for the North American (b) and Eurasian ice sheet (c). The different curves correspond to the six different AGCM: ECHAM3 (black line), UGAMP (red line), GENESIS2 (green line), CCSR1 (blue line), LMD5 (purple line), MRI2 (grey line). The dashed line represents the ice-equivalent sea-level contribution of the Northern hemisphere (see text).

Title Page

Abstract

Introduction

Conclusions

References

Tables

Figures

◀

▶

◀

▶

Back

Close

Full Screen / Esc

Printer-friendly Version

Interactive Discussion

Ice-sheet evolution during the last climatic cycle

S. Charbit et al.

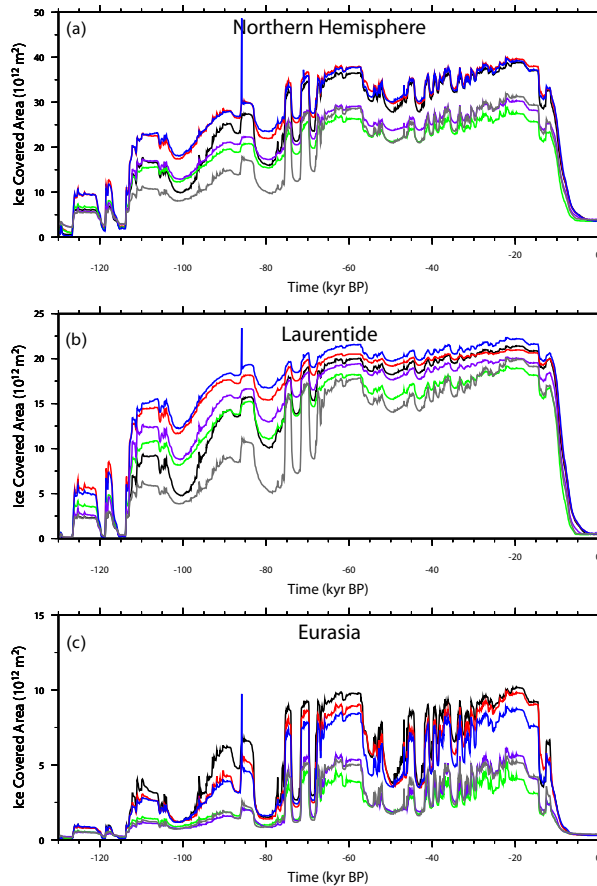


Fig. 9. Same as Fig. 2 but for the ice-covered area.

Title Page

Abstract

Introduction

Conclusions

References

Tables

Figures

◀

▶

◀

▶

Back

Close

Full Screen / Esc

Printer-friendly Version

Interactive Discussion